Research Article | Vol. 12, No. 12 / 1 Dec 2022 / Optical Materials Express 4574

Optical Materials EXPRESS

# Humidity-induced direct modification of the optical response of plasmonic nanorod metamaterials

YUNLU JIANG,[1,*] ALEXEY V. KRASAVIN,[1] MAZHAR E. NASIR,[1] PAN WANG,[2] AND ANATOLY V. ZAYATS[1]

[1]Department of Physics and London Center for Nanotechnology, King's College London, Strand, London WC2R 2LS, UK
[2]State Key Laboratory of Modern Optical Instrumentation, College of Optical Science and Engineering, Zhejiang University, Hangzhou 310027, China
[*]yunlu.jiang@kcl.ac.uk

**Abstract:** Plasmonic nanorod metamaterials are often used as a high-performance optical sensing platform for the detection of biochemical and gas species. Here, we investigate the effect of environmental humidity on their optical response. Due to the high refractive index sensitivity, a significant change in the transmission is observed with $\Delta T/T$ reaching values of more than 5% when the relative humidity is changed from 11% to 75%. This is the result of the condensation of water molecules on a rough surface of the gold nanorods. This finding reveals the importance of protecting plasmonic nanostructures from relative humidity variations in many practical applications. By coating the nanorods with a monolayer of poly-L-histidine, the fractional change of transmission is doubled due to the hydrophilic property of the monolayer, which can be used for the development of high-sensitivity relative humidity and dew condensation sensors.



## 1. Introduction

In the past decades, plasmonic metamaterials, artificial optical materials consisting of periodically or randomly arranged plasmonic nanostructures, have been widely investigated since they offer a unique means to engineer optical properties beyond those occurring in nature to achieve exotic optical phenomena, such as magnetism at high frequencies [1] and negative refraction [2,3]. They have opened up opportunities for numerous applications in nanophotonics, e.g. superlensing [4,5], optical cloaking [6,7], and nonlinear optics [8,9]. Among them, plasmonic nanorod metamaterials consisting of arrays of strongly interacting, aligned plasmonic nanorods are particularly interesting. They have been successfully employed for a variety of applications, ranging from imaging beyond the diffraction limit [10], enhancement of optical nonlinearities [11], spontaneous emission control and lasing [12–14] to biochemical sensing [15], nanoscale optomechanics [16] and tunneling-based plasmon excitation [17–19]. Particularly, because the optical properties (e.g., extinction, transmission, and reflection spectra) of a plasmonic nanorod metamaterial are determined not only by the plasmonic response of the individual nanorods in the metamaterial, but also by the electromagnetic coupling between them, they are extremely sensitive to the refractive index changes in the surrounding dielectric environment. A record-high refractive index sensitivity of $\sim 4 \times 10^4$ nm/RIU [15,20] reveals the nanorod metamaterials as an attractive platform for the development of high-sensitivity optical sensors.

In many applications (e.g., gas sensing, linear and nonlinear photonics), nanorods of the metamaterials (bare or functionalized) are directly exposed to an ambient environment, which *a priori* has certain relative humidity (RH). Due to the extremely high sensitivity of nanorod

#469414 https://doi.org/10.1364/OME.469414
Journal © 2022 Received 5 Jul 2022; revised 23 Aug 2022; accepted 23 Aug 2022; published 14 Nov 2022

Optical Materials EXPRESS

metamaterials to the refractive index of their surroundings, a change in the RH of the environment may cause a direct change in the optical response of the metamaterials and subsequently affect their application performance. Therefore, it is important to reveal the effect of RH of the environment on the optical properties of the nanorod metamaterials, which we demonstrate in this work. We show that a fractional change of up to 5.3% in transmission occurs for a bare gold nanorod metamaterial when it is exposed to an environment with the RH changing from 11% to 75%, which is attributed to the condensation of water molecules on a rough surface of the nanorods (Fig. 1(a)). This change can get almost doubled if a monolayer of hydrophilic polymer, such as poly-L-histidine (PLH), is coated onto the nanorods, providing an opportunity to develop metamaterial-based humidity sensors.

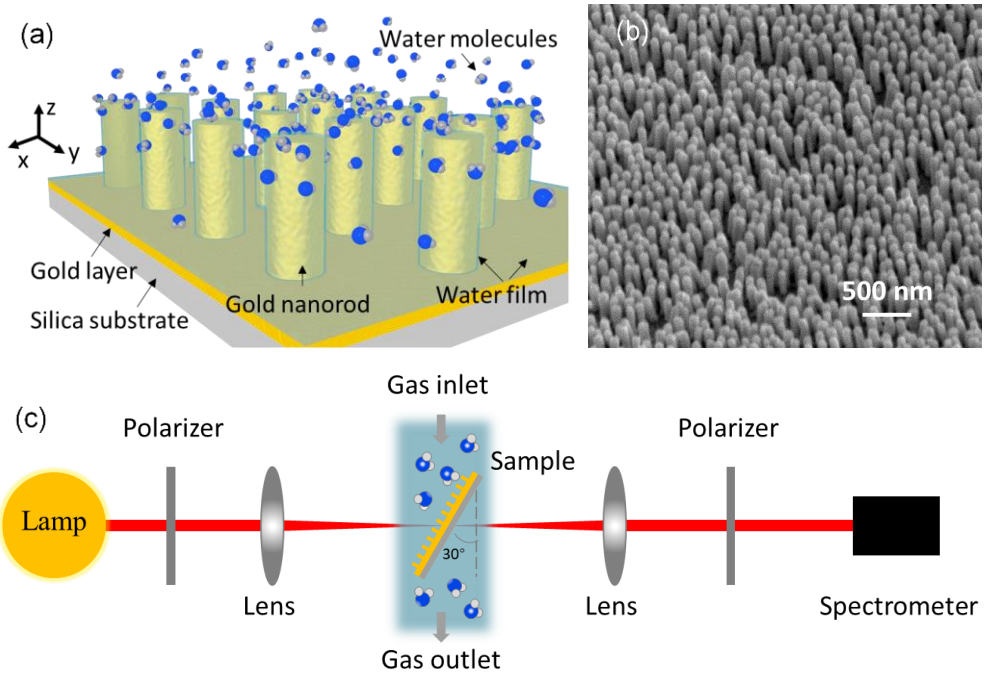


**Fig. 1.** (a) Schematic diagram showing condensation of water molecules onto the surface of freestanding gold nanorods in the metamaterial. (b) SEM image of the bare gold nanorod metamaterial. (c) Experimental apparatus used for studying the effect of environmental humidity on the optical response of the gold nanorod metamaterials.

## 2. Methods

### *2.1. Fabrication of gold nanorod metamaterials*

Gold nanorod metamaterial was fabricated by direct electrodeposition of gold into a substrate-supported porous anodized aluminum oxide (AAO) template [21]. The substrate is a multilayered structure comprised of a glass slide, a tantalum oxide adhesive layer (~10 nm in thickness) and a gold film (~7 nm in thickness). An aluminum film is then deposited on the substrate, and subsequently anodized (in 0.3 M oxalic acid at 40 V) to produce the AAO template with naturally produced nanoscale pores. The length of the rods can be, therefore, controlled by changing the thickness of the initial aluminum film. The spacing and diameter of the pores are defined by the anodization conditions. Finally, gold nanorod metamaterial embedded in the alumina matrix was obtained by electrodeposition of gold into the AAO pores, the thin gold film works in this case as

Optical Materials EXPRESS

an electrode. Gold nanorods were first overgrown to fully fill the AAO pores, and then the sample was ion-milled to remove the overgrown gold layer on the surface and annealed at 200 °C for 2 h. To expose the nanorods for sensing applications, the alumina matrix was chemically etched by putting the as-fabricated nanorod metamaterial into an aqueous solution of 3.5% $H_3PO_4$ at 35 °C, resulting in a freestanding gold nanorod array (in the following addressed as a bare nanorod array). Figure 1(b) shows a typical scanning electron microscopy (SEM) image of the bare gold nanorod metamaterial, in which high-density freestanding gold nanorods on a substrate can be observed. The average diameter, length and separation of the nanorods in the assembly we measured to be approximately 50, 230 and 100 nm, respectively.

A PLH-coated gold nanorod array was further obtained via a molecular self-assembly approach [19]. In brief, a PLH solution was first prepared by dissolving ~5 mg of a PLH powder into 5 mL of deionized water with its pH adjusted to 5–6 using 0.1 M HCl. A bare gold nanorod array was then immersed into the PLH solution for ~30 min. Due to the high affinity of the functional groups of PLH to gold, a monolayer of PLH layer was self-assembled on the gold nanorod surface. After rinsing with deionized water and dried under a $N_2$ flow, the PLH-coated nanorod array was obtained.

### 2.2. Experimental apparatus

In order to study the effect of environmental humidity on the optical response of gold nanorod metamaterials, the metamaterials (bare and PLH-functionalized nanorod arrays) were placed in a custom-designed airtight chamber with transparent windows (Fig. 1(c)). A nitrogen gas of different humidity (controlled by varying the amount of humid and dry nitrogen in their mixture, monitored by a commercial hygrometer) was introduced into the chamber at a flow rate of about 1 L/min. Collimated transverse magnetic (TM) polarized white light from a tungsten-halogen lamp illuminated the metamaterial at an angle of incidence of 30°, and the transmission was monitored with a spectrometer (QE Pro, Ocean Optics). All measurements were conducted at room temperature and atmospheric pressure.

### 2.3. Numerical simulations

Numerical simulations were performed using the finite element method (COMSOL Multiphysics software). A hexagonal array of gold nanorods was simulated. Using the symmetry of the system, a unit cell of the array was modelled with the Floquet boundary conditions implementing the appropriate phase shift for the parallel pairs of the side boundaries. The top boundary of the air domain above the metamaterial, and the bottom boundary of the substrate domain below the metamaterial were set to have scattering boundary conditions, with the top boundary acting as the source boundary for the incident plane electromagnetic wave. At the top and the bottom of the overall simulation domain, perfectly matched layers were implemented to avoid back-reflection. Below the nanorods, a 10 nm $Ta_2O_5$ and a 7 nm Au layers were introduced in order to represent the structure of the experimental sample. The nanorods were modelled as ideal cylinders, with a water layer of the thickness from 0 to 0.7 nm uniformly covering them and the top of the gold layer below. The optical properties of the materials were taken from literature: Au [22], $Ta_2O_5$ [23], $SiO_2$ [24]. Additionally, the permittivity of Au in the nanorods was modified to implement a restricted mean free path of the electrons of 3 nm, reflecting smaller grain sizes obtained in the electrodeposition fabrication process [25,26].

The optical properties of nanoscale water have recently been intensively investigated [27]. Theoretical estimations of the optical response of molecular layers of water requires first-principle simulations of a particular system in particular conditions. However continuous refractive index models have been also successfully applied. Following the recent approach [28], a bulk non-dispersive refractive index was used for water layer, equal to 1.33.

Optical Materials EXPRESS

The optical response of the bare gold nanorod metamaterials is presented in Fig. 2(a) (black curve). The spectrum is dominated by a transmission dip around the wavelength of 500 nm and a humidity-dependent shoulder at around 650 nm. The dip corresponds to the excitation of the transverse plasmonic resonance of the coupled nanorods spectrally overlapping with an ENZ wavelength region [29]. This can be easily understood looking at the spectral dependence of the effective permittivity of the metamaterial (Fig. 2(b)). The transverse resonance corresponds to the peak of the imaginary part of the transverse permittivity components $\mathrm{Im}(\varepsilon_{xx,yy})$ and, for these nanorod parameters, spectrally overlaps the metamaterial opacity region at the ENZ condition at the wavelength slightly above 500 nm. Overall, this produces a combined transmission dip at the spectral position which is in excellent agreement with the experiments. The shoulder in a 600–650 nm spectral region appearing in humidity measurements (Fig. 3(a)) is related to the excitation of a Fabry-Perot (FP) mode supported by the metamaterial slab [30]. The presence of the FP mode was additionally confirmed with a matching dip in the reflection spectrum. After the PLH coating, there is an appreciable difference in the optical transmission compared to the bare nanorod metamaterial due to the high sensitivity of the nanorod metamaterial to the refractive index changes (Fig. 2(a)).

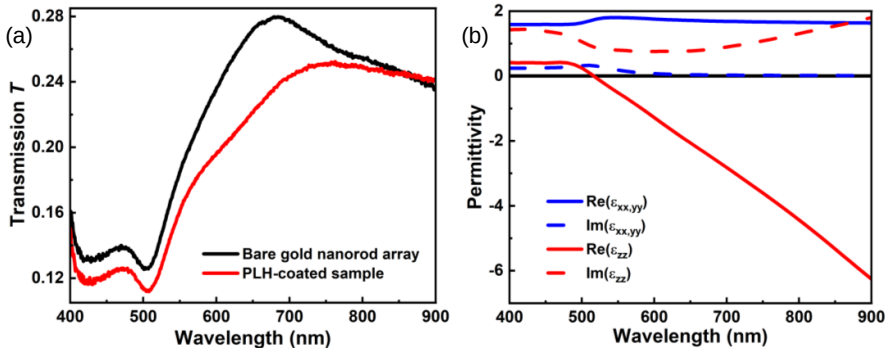


**Fig. 2.** (a) The experimental transmission spectra for bare and PLH-coated metamaterials in a dry nitrogen atmosphere. (b) The spectra of the effective permittivity of the bare metamaterial calculated using an effective medium theory [30]. The metamaterial parameters are: nanorod diameter 50 nm, nanorod length 230 nm and inter-rod separation 100 nm.

## 3. Results and discussion

The optical response of the bare gold nanorod metamaterial to the environmental humidity was investigated. With the increase of RH, an obvious change in the optical transmission spectra is observed, predominantly in a wavelength range of 600–700 nm (Fig. 3(a)). This is highlighted by plotting a relative change $\Delta T/T$ (Fig. 3(b)), from where one can see an overall drop across the entire measured spectral range as RH increases, with the maximum drop at around 610 nm (~5.3% under RH of 75%). This spectral position is close to that of the FP mode of the sample, which has been demonstrated to be extremely sensitive to refractive index changes in the surrounding dielectric environment of the nanorods [15,31].

Since the change in the refractive index of air with varied RH is very small ($4.2 \times 10^{-7}$ for a RH change from 0 to 50% [32]), the obvious change in the transmission is not likely caused by the change in the refractive index of the surrounding humid nitrogen gas. Also, because the experiment was conducted at room temperature (25 °C) and the highest RH was less than 80%, the nanorod metamaterial was operated above the dew point (24 °C) and, therefore, there is no macroscopic dew formed on the nanorod array. The obvious change in the transmission of the

Optical Materials EXPRESS

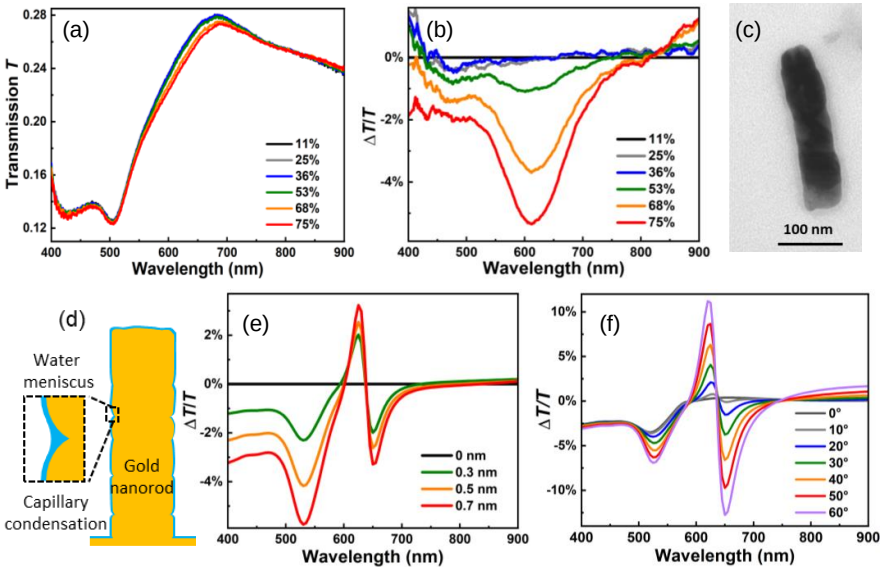


**Fig. 3.** (a) Transmission spectra measured at a 30° angle of incidence and (b) corresponding relative intensity change $\Delta T/T$ when the bare gold nanorod metamaterial is exposed to various levels of RH (11–75%). (c) TEM image of a single gold nanorod (after detachment from the array) showing the rough surface of the nanorods. (d) Schematic diagram of capillary condensation at the rough surface. (e) Numerically simulated transmission through the metamaterial with the gold nanorods and bottom gold surface covered with a thin layer of water molecules with a uniform thickness indicated in the legend. (f) Numerically simulated relative transmission change $\Delta T/T$ as a function of the incidence angle (0-60°), when bare gold nanorods are covered with a 0.7 nm $H_2O$ layer.

bare nanorod metamaterial with increasing RH is mainly due to nanoscale water condensation on the rough surface of the polycrystalline gold nanorods. As indicated by a transmission electron microscopy (TEM) image of a gold nanorod detached from the metamaterial (Fig. 3(c)), the surface of the nanorods is rough and has a lot of grooves (with dimensions at a nanometer scale) produced by the gold grains. Therefore, with moisture introduced into the chamber, in addition to the condensation of water on the smooth surface of the grains, capillary water condensation (Fig. 3(d)) in the grooves forms a water meniscus with an increased nonuniform nanoscale thickness [33,34]. Additionally, continuous water layers can condensate at the top of the nanorods and the bottom gold layer.

To confirm experimental findings, numerical simulations of the system were performed. By using an average water film thickness of 0.3, 0.5, and 0.7 nm on each nanorod, two obvious dips around 530 and 650 nm can be observed in the spectral dependence of $\Delta T/T$ with the increase of the water film thickness (Fig. 3(e)), indicating the high sensitivity of the transmission to the condensation of water molecules. The simulation results show the same general trend in the transmission changes, while the difference with the experimental spectra can be expected due to a much more complex structure of the condensation on the electrodeposited gold nanorods, compared to a uniform layer on the surface of smooth nanorods considered in the numerical simulations. The general trend also shows that the humidity-induced transmission change can increase with the increase of the incidence angle (Fig. 3(f)).

For the PLH-coated gold nanorod array, the transmission spectrum shows a similar dependence on the environmental RH changes (Fig. 4(a)), but with a larger value of $\Delta T/T$, (~9.3% under a

Optical Materials EXPRESS

RH of 75%; Fig. 4(b)). Figure 4(c) further presents the RH-dependent $\Delta T/T$ of the bare and PLH-coated gold nanorod arrays plotted at the wavelength of 613 and 640 nm, respectively, with the RH increasing and decreasing in the range between 11 to 75%. For both curves, in the range of low RH (11–36%), a little change can be observed (the slopes are 0.002 for the bare and 0.003 for the PLH-coated nanorod metamaterials). For the middle RH ange (36–53%), a gradual change (the slopes are 0.041 for bare and 0.086 for PLH-coated nanorod metamaterials) is present. For the higher humidity values (53–75%), one can see a much steeper slopes for all the curves: 0.191 for bare and 0.319 for PLH-coated nanorod metamaterials, indicating a higher sensitivity response for higher humidity values. Moreover, compared with the bare gold nanorod array (black curve), the PLH-coated counterpart (red curve) shows about a two-fold higher sensitivity, as a steeper slope can be seen across the entire humidity range. This is attributed to the hydrophilic properties of the PLH monolayer deposited onto the nanorod surface, which can absorb more water molecules than the surface of the bare gold nanorod arrays where water molecules absorbed only due to condensation. The RH-dependent fractional changes in the transmission, measured under decreasing RH, agrees well with those measured under increasing RH, indicating physisorption of water molecules on the metamaterial and good reversibility of the sensor operation.

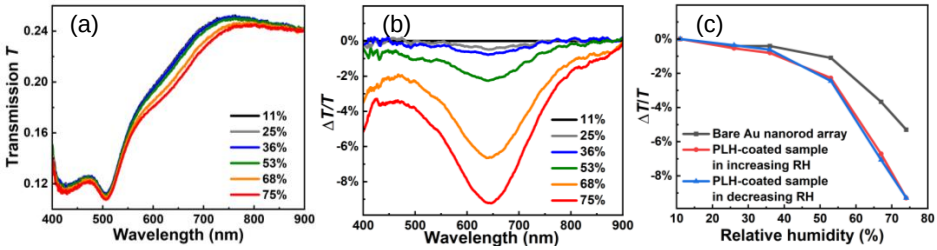


**Fig. 4.** (a) Transmission spectra and (b) the corresponding relative intensity change $\Delta T/T$ when the PLH-coated gold nanorod metamaterial was exposed to nitrogen gas with various RH (11–75%). (c) Comparison of the relative intensity variation $\Delta T/T$ with the change of the environmental humidity measured at 613 and 640 nm wavelength for the bare and PLH-coated gold nanorod metamaterials, respectively.

## 4. Conclusion

We have demonstrated a strong dependence of an optical response of a freestanding gold nanorod metamaterial on the changes in the RH of the environment due to roughness-assisted nanoscale condensation of water on the nanorod surfaces. This reveals the importance of considering the humidity conditions in the optical characterization of the plasmonic nanostructures and most importantly in their practical applications in sensing. The sensitivity to RH was further improved by functionalizing the metamaterial nanorods with a monolayer of hydrophilic PLH polymer promoting the adsorption of water molecules, which opens a prospective for the development of such metamaterial platform for optical humidity sensors. Particularly, the PLH-functionalized nanorod metamaterials shown almost a 9% change in the transmission with the relative humidity change from 11 to 75%, underlined by the high sensitivity of the excitation of the FP modes supported by the metamaterial layer to the changes in the environment.

**Funding.** Engineering and Physical Sciences Research Council (EP/M013812/1, EP/W017075/1); European Research Council iCOMM (789340); China Scholarship Council.

**Disclosures.** The authors declare no conflicts of interest.

**Data availability.** All the data supporting finding of this work are presented in the Results section and are available from the corresponding author.

Optical Materials EXPRESS

## References


1. T. J. Yen, W. J. Padilla, N. Fang, D. C. Vier, D. R. Smith, J. B. Pendry, D. N. Basov, and X. Zhang, "Terahertz magnetic response from artificial materials," Science **303**(5663), 1494–1496 (2004).
2. V. M. Agranovich, Y. R. Shen, R. H. Baughman, and A. A. Zakhidov, "Linear and nonlinear wave propagation in negative refraction metamaterials," Phys. Rev. B. **69**(16), 165112 (2004).
3. J. Yao, Z. Liu, Y. Liu, Y. Wang, C. Sun, G. Bartal, A. M. Stacy, and X. Zhang, "Optical negative refraction in bulk metamaterials of nanowires," Science **321**(5891), 930 (2008).
4. A. Salandrino and N. Engheta, "Far-field subdiffraction optical microscopy using metamaterial crystals: Theory and simulations," Phys. Rev. B. **74**(7), 075103 (2006).
5. Z. Jacob, L. V. Alekseyev, and E. Narimanov, "Optical hyperlens: Far-field imaging beyond the diffraction limit," Opt. Express **14**(18), 8247 (2006).
6. Y. Lai, H. Chen, Z.-Q. Zhang, and C. T. Chan, "Complementary media invisibility cloak that cloaks objects at a distance outside the cloaking shell," Phys. Rev. Lett. **102**(9), 093901 (2009).
7. W. Cai, U. K. Chettiar, A. V. Kildishev, and V. M. Shalaev, "Optical cloaking with metamaterials," Nat. Photonics **1**(4), 224–227 (2007).
8. M. Kauranen and A. V. Zayats, "Nonlinear plasmonics," Nat. Photonics **6**(11), 737–748 (2012).
9. G. A. Wurtz, R. Pollard, W. Hendren, G. P. Wiederrecht, D. J. Gosztola, V. A. Podolskiy, and A. V. Zayats, "Designed ultrafast optical nonlinearity in a plasmonic nanorod metamaterial enhanced by nonlocality," Nat. Nanotechnol. **6**(2), 107–111 (2011).
10. P. Segovia, G. Marino, A. V. Krasavin, N. Olivier, G. A. Wurtz, P. A. Belov, P. Ginzburg, and A. V. Zayats, "Hyperbolic metamaterial antenna for second-harmonic generation tomography," Opt. Express **23**(24), 30730 (2015).
11. G. Marino, P. Segovia, A. V. Krasavin, P. Ginzburg, N. Olivier, G. A. Wurtz, and A. V. Zayats, "Second-harmonic generation from hyperbolic plasmonic nanorod metamaterial slab," Laser Photonics Rev. **12**(2), 1700189 (2018).
12. P. Ginzburg, D. J. Roth, M. E. Nasir, P. Segovia, A. V. Krasavin, J. Levitt, L. M. Hirvonen, B. Wells, K. Suhling, D. Richards, V. A. Podolskiy, and A. V. Zayats, "Spontaneous emission in non-local materials," Light: Sci. Appl. **6**(6), e16273 (2017).
13. D. J. Roth, A. V. Krasavin, A. Wade, W. Dickson, A. Murphy, S. Kéna-Cohen, R. Pollard, G. A. Wurtz, D. Richards, S. A. Maier, and A. V. Zayats, "Spontaneous emission inside a hyperbolic metamaterial waveguide," ACS Photonics **4**(10), 2513–2521 (2017).
14. R. Chandrasekar, Z. Wang, X. Meng, S. I. Azzam, M. Y. Shalaginov, A. Lagutchev, Y. L. Kim, A. Wei, A. V. Kildishev, A. Boltasseva, and V. M. Shalaev, "Lasing action with gold nanorod hyperbolic metamaterials," ACS Photonics **4**(3), 674–680 (2017).
15. A. V. Kabashin, P. Evans, S. Pastkovsky, W. Hendren, G. A. Wurtz, R. Atkinson, R. Pollard, V. A. Podolskiy, and A. V. Zayats, "Plasmonic nanorod metamaterials for biosensing," Nat. Mater. **8**(11), 867–871 (2009).
16. P. Ginzburg, A. V. Krasavin, A. N. Poddubny, P. A. Belov, Y. S. Kivshar, and A. V. Zayats, "Self-induced torque in hyperbolic metamaterials," Phys. Rev. Lett. **111**(3), 036804 (2013).
17. A. V. Krasavin, P. Wang, M. E. Nasir, Y. Jiang, and A. V. Zayats, "Tunneling-induced broadband and tunable optical emission from plasmonic nanorod metamaterials," Nanophotonics **9**(2), 427–434 (2020).
18. P. Wang, M. E. Nasir, A. V. Krasavin, W. Dickson, and A. V. Zayats, "Optoelectronic synapses based on hot-electron-induced chemical processes," Nano Lett. **20**(3), 1536–1541 (2020).
19. P. Wang, A. V. Krasavin, M. E. Nasir, W. Dickson, and A. V. Zayats, "Reactive tunnel junctions in electrically driven plasmonic nanorod metamaterials," Nat. Nanotechnol. **13**(2), 159–164 (2018).
20. R. Yan, T. Wang, X. Yue, H. Wang, Y.-H. Zhang, P. Xu, L. Wang, Y. Wang, and J. Zhang, "Highly sensitive plasmonic nanorod hyperbolic metamaterial biosensor," Photonics Res. **10**(1), 84 (2022).
21. W. Dickson, G. A. Wurtz, P. Evans, D. O'Connor, R. Atkinson, R. Pollard, and A. V. Zayats, "Dielectric-loaded plasmonic nanoantenna arrays: a metamaterial with tuneable optical properties," Phys. Rev. B. **76**(11), 115411 (2007).
22. P. B. Johnson and R. W. Christy, "Optical constant of the noble metals," Phys. Rev. B **6**(12), 4370–4379 (1972).
23. L. V. Rodríguez-de Marcos, J. I. Larruquert, J. A. Méndez, and J. A. Aznárez, "Self-consistent optical constants of $SiO_2$ and $Ta_2O_5$ films," Opt. Mater. Express **6**(11), 3622 (2016).
24. I. H. Malitson, "Interspecimen comparison of the refractive index of fused silica," J. Opt. Soc. Am. **55**(10), 1205 (1965).
25. P. H. Lissberger and R. G. Nelson, "Optical properties of thin film Au-$MgF_2$ cermets," Thin Solid Films **21**(1), 159–172 (1974).
26. R. J. Pollard, A. Murphy, W. R. Hendren, P. R. Evans, R. Atkinson, G. A. Wurtz, A. V. Zayats, and V. A. Podolskiy, "Optical nonlocalities and additional waves in epsilon-near-zero metamaterials," Phys. Rev. Lett. **102**(12), 127405 (2009).
27. T. H. H. Le, A. Morita, and T. Tanaka, "Refractive index of nanoconfined water reveals its anomalous physical properties," Nanoscale Horiz. **5**(6), 1016–1024 (2020).
28. M. Douas, M. I. Marqués, and P. A. Serena, "Identification of water content in nanocavities," Nanoscale Res. Lett. **8**(1), 171 (2013).
29. P. Wang, M. E. Nasir, A. V. Krasavin, W. Dickson, Y. Jiang, and A. V. Zayats, "Plasmonic metamaterials for nanochemistry and sensing," Acc. Chem. Res. **52**(11), 3018–3028 (2019).

Optical Materials EXPRESS

30. N. Vasilantonakis, M. E. Nasir, W. Dickson, G. A. Wurtz, and A. V. Zayats, "Bulk plasmon-polaritons in hyperbolic nanorod metamaterial waveguides," Laser Photonics Rev. **9**(3), 345–353 (2015).
31. N. Vasilantonakis, G. A. Wurtz, V. A. Podolskiy, and A. V. Zayats, "Refractive index sensing with hyperbolic metamaterials: strategies for biosensing and nonlinearity enhancement," Opt. Express **23**(11), 14329 (2015).
32. P. E. Ciddor, "Refractive index of air: new equations for the visible and near infrared," Appl. Opt. **35**(9), 1566–1573 (1996).
33. H. E. Limodehi and F. Légaré, "Fiber optic humidity sensor using water vapor condensation," Opt. Express **25**(13), 15313 (2017).
34. N. Gupta, H. M. Fahad, M. Amani, X. Song, M. Scott, and A. Javey, "Elimination of response to relative humidity changes in chemical-sensitive field-effect transistors," ACS Sens. **4**(7), 1857–1863 (2019).